`

# Improving Hypoxia Forecast within the Chesapeake Bay by refining a Primary Production Model

Sergey Dutt
Luther College
Dante M.L. Horemans, Pierre St-Laurent, &
Marjorie A.M. Friedrichs
2 August 2024

`

## Synopsis

To improve the hypoxia forecasts generated by the operational Chesapeake Bay Environmental Forecast System (https://www.vims.edu/cbefs), we study its primary production (PP) model with the ultimate goal of improving its performance. We calibrate variations of the current PP model (e.g., temperature dependence and nutrient limitation) to a multi-decadal PP data set of the Chesapeake Bay. Calibrating these models to specific salinity regions and seasons shows that although the optimal model parameters may be different for these times and locations, it does not necessarily result in a better model skill.


## Abstract

The Chesapeake Bay typically experiences hypoxia (< 2 or 3 mg $O_2$ $L^{-1}$) between May and October in its upper main channel and tributaries. Stakeholders such as anglers and oyster farmers are interested in forecasts of hypoxia because it shrinks habitats and disrupts trophic structures. The Chesapeake Bay Environmental Forecast System (CBEFS) was thus developed to provide daily forecasts of hypoxia in the Bay. To further improve the accuracy of the forecasts, we explored alternative implementations of the PP model used in CBEFS. PP is the rate that inorganic carbon is converted into organic biomass, and may cause hypoxia, because the biomass produced at the surface ultimately sinks to the bottom and dies where it can lead to an increase in bacterial respiration. In this study we used an extensive Chesapeake Bay PP data set to calibrate versions of our current PP model (i.e., alternative nutrient limitation and temperature dependence in growth rate) across different seasons and four salinity regions. Three metrics (correlation, bias, and root relative squared difference) are used to compare the skill of these various PP models. We hypothesize that the various seasons and salinity regions are associated with different optimal model parameter values and skill because of their unique phytoplankton characteristics. While the optimal parameter values did differ across seasons and regions, the model skill usually did not change between the current and alternative model. Thus, we did not find strong indicators for changing our temperature and nutrient dependence in the current PP model of CBEFS.


## Introduction

The Chesapeake Bay is the largest estuary in the continental U.S, and its nutrient loadings to the Bay have approximately doubled between 1940 and 1990 because of its

`

large watershed (approximately 15 times the size of the bay) that contains expanding cities and increasing agricultural land use (Hagy *et al.,* 2004; Kemp *et al.,* 2005). The resulting high nutrient concentrations, called eutrophication, is a prevailing problem within the Bay because it may lead to hypoxia. Hypoxia occurs when the water's dissolved oxygen (DO) concentration is low enough to harm aquatic life (Nixon, 1995; Hagy *et al.,* 2004). Different marine species have distinct DO thresholds, but hypoxia is generally defined as less than 2 or 3 mg $O_2$ $L^{-1}$(Batiuk, 2002). Such low DO waters are concerning because they shrink habitats and disrupt trophic structures, decreasing the diversity, productivity, and resilience within the Chesapeake Bay (Seitz *et al.,* 2009).

Hypoxia in the Chesapeake Bay follows a specific spatial and seasonal pattern. The Bay is most hypoxic in the deepest portions of the Bay and its tributaries (most notably in the main channels of the mainstem and Potomac River) during the summer (Fig. 1). Hypoxic conditions typically begin around May and end around October (St-Laurent and Friedrichs, 2024; Fig. 2). The reasons are that warm temperatures decrease the solubility of DO, and also increase biological activity and respiration (Diaz and Rosenberg, 2008; Irby *et al*., 2018). Biological activity is usually a prerequisite to hypoxia because bacteria consuming organic matter deoxygenate the water (Kemp *et al.,* 2005). This means that hypoxia is partially reliant on the increase of organic matter within the Bay, which can occur from organic matter entering the Bay, or an increase in primary production (PP): the rate that inorganic carbon is converted into organic biomass (Chavez *et al.,* 2010).

PP is a complex mechanism that relies on many factors such as temperature, light, organic matter, nitrate ($NO_3$), ammonium ($NH_4$), and phosphate (Cloern*,* 2001; Harding Jr *et al*., 1986). Given this complexity, numerical models are useful tools for understanding production because they can distinguish the various constraints limiting PP. The current version of CBEFS uses the 3-D Regional Ocean Modeling System (ROMS) with the Estuarine Carbon Biogeochemistry (ECB) model and reproduces bottom DO concentrations relatively well in the Chesapeake Bay (Fig. 2; St-Laurent and Friedrichs, 2024; Bever *et al.,* 2021). The observations (gray dots) mostly align with the modeling data (blue line) at station CB3.2 (Fig. 2A). Focusing on station LE3.6, the model performs well between January and March, but slightly

`

underestimates the bottom DO between April and July (Fig. 2B). The model skill thus varies in time and space.

Our objective is to perform an extensive model sensitivity study in order to obtain insight into model skill varying in time and space, focusing on PP. We calibrate PP models with varying model complexity to a multi-decadal PP data set of the Chesapeake Bay. Calibrating these models to specific regions and seasons allowed us to compare the optimal model parameters and model skill for these times and locations. This approach guides us in determining which parameters and model assumptions in the current PP model may explain the variability of the model skill (Fig. 2) We hypothesize that various seasons and regions in the Chesapeake Bay are associated with unique phytoplankton characteristics that may require their own set of model assumptions to further improve the hypoxia forecasts from CBEFS and decrease the variability of the model skill in time and space.

## Methods

In order to test our hypothesis, we separated data into seasons (i.e., winter, spring, summer, and fall) and salinity regions: freshwater (salinity < 0.5), oligohaline (0.5 ≤ salinity < 5), mesohaline (5 ≤ salinity <18), and polyhaline (salinity ≥ 18), which when combined with the four seasons creates sixteen different combinations.

The PP data came from the Chesapeake Bay Program and contained over 13,000 observations that cover the tributaries and main channel of the Chesapeake Bay between 1984-2009. These data correspond to Carbon 14 ($^{14}C$) isotope incubation experiments under saturated light conditions. We paired the $^{14}C$ PP data with corresponding environmental *in situ* observations based on location, date, and water depth. We used the data and a nonlinear least squares regression [*nls()* package from the R software; version 4.4.0; 2024-04-24] to calibrate alternative versions of the current PP model of CBEFS that includes four components: a temperature dependence of maximum growth rate, nitrogen limitation, respiration, and phytoplankton abundance (Model 1):

$$\partial_t P = \underbrace{\mu_{max}}_{\substack{maximum\\ growth\\ rate}} \underbrace{(1-\gamma_P)}_{respiration} \underbrace{\left(L_{NO_3}+L_{NH_4}\right)}_{\substack{nitrogen\\ limitation}} \underbrace{P}_{\substack{phytoplankton\\ abundance\\ approximated\ by\\ C:Chl-a*Chl-a}}, \quad (1)$$

in which $P$ is the phytoplankton abundance, $\gamma p$ (i.e.., 0.07) is a constant respiration, Chla is the Chlorophyll-a (Chla) concentration, and C:Chla is the carbon to Chla ratio. Phosphorus is assumed to not be limiting.

`

The maximum algal growth rate $\mu_{max}$ (in units of $d^{-1}$) and nutrient limitation functions $L_{NO3}$ and $L_{NH4}$ are:

$$\mu_{max}(T) = \max [4 , 0.55e^{\psi_{pmax}*T}], \quad (2)$$

$$L_{NO_3} = \frac{NO_3}{NO_3 + K_{NO_3}} \frac{1}{1 + {NH_4}/{K_{NH_4}}}, \quad (3)$$

$$L_{NH_4} = \frac{NH_4}{NH_4 + K_{NH_4}}. \quad (4)$$

Equation (2) assumes a growth rate of 4 $d^{-1}$, except at very high temperatures, where $\psi_{pmax}$ (i.e.., 0.08065 $^oC^{-1}$) is the temperature dependence for maximum photosynthetic growth rate. Equation (3) is the $NO_3$ limitation that has an inhibition of $NO_3$ uptake by $NH_4$ (Parker, 1993), and Eq. (4) is the $NH_4$ limitation. In Eqs. (3) and (4), $NO_3$ is nitrate concentration, $NH_4$ is ammonium concentration, $K_{NO_3}$ (0.5 mmol-N $m^{-3}$) is the half-saturation constant for $NO_3$ uptake, and $K_{NH_4}$(0.5 mmol-N $m^{-3}$) is the half-saturation constant for $NH_4$ uptake.

In our first model experiment, we consider an alternative implementation of the maximum algal growth rate based on the Eppley Model (Eppley, 1971; Model 2):

$$\mu_{max}(T) = \mu_{00}\, \mu_{01}^{T}, \quad (5)$$

where $\mu_{00}$ (i.e., 0.97 $d^{-1}$) is the maximum growth rate at 0 $^oC$ and $\mu_{01}$ (i.e., 1.03) is the calibration parameter in temperature dependence for $\mu_{max}$. In the second model experiment, we focus on the nitrogen limitation (i.e., $L_{NO_3} + L_{NH_4}$) and tune the values for $K_{NO_3}$ and $K_{NH_4}$ in Model 1 to their optimal values (Fig. 3).

In order to obtain realistic values, we require $K_{NO3}$ and $K_{NH4}$ to be between 0 and 5 mmol-N $m^{-3}$. We also created a function that generated random start values within a realistic range for all of the parameters we were tuning (i.e., C:Chla, $K_{NO_3}$, and $K_{NH_4}$) and implemented the function in *nls()* to run up to 200 times, only accepting start values that lead to convergence. This ensured that we obtained the overall minimal cost function value for each parameter, and not just a local minimum.

In all of the model calibration experiments, C:Chla ratios are tuned to its optimal value. We allow C:Chla to change since it is light and species dependent and may thus vary across seasons and regions of the Bay because of seasonal changes in daylength and spatial variability in water turbidity (Cerco et al., 2004). To evaluate whether the different parameter values improved the model, we calculated the model skill for each model experiment using the following metrics: correlation, bias, and root-relative squared difference (RRSD).

`

These metrics were implemented using the *Metrics* package in R:

$$r = \frac{\sum_{i=1}^{n}(O_i - \bar{O})(P_i - \bar{P})}{\sqrt{\sum_{i=1}^{n}(O_i - O)^2 \sum_{i=1}^{n}(P_i - P)^2}}, \quad (6)$$

$$bias = \frac{\sum_{i=1}^{n}(P_i - O_i)}{n} = \bar{P} - \bar{O}, \quad (7)$$

$$RRSD = \sqrt{\frac{\sum_{i=1}^{n}(P_i - O_i)^2}{\sum_{i=1}^{n}(P_i - \bar{P})^2}}, \quad (8)$$

where $\bar{y} = \frac{1}{n}\sum_{i=1}^{n} P_i$.

In Eqs. (6-8), $n$ is the number of observations, $O_i$ is the $i$th of $n$ observations, $P_i$ is the $i$th of $n$ model prediction, $\bar{O}$ is the observation averages, and $\bar{P}$ is the model prediction averages. The correlation coefficient, $r$, shows the extent that the model predictions are linearly related to the observations, with a range of -1 to 1, where the limits are a complete correlation and 0 is no correlation. Bias and RRSD both measure differences between observations and model predictions, where values closer to zero indicate better model performance. In order to account for variability in each metric, we used bootstrapping to resample the data and calibrate each model 200 times and calculated the standard deviation in the model skill out of those 200 resamples.

**Results**

Beginning with the environmental observations from the data set, we see a seasonal pattern in temperature, PP, and Chla (Fig. 4). For example, all four regions have a higher temperature in the summer than in spring or fall, and PP in freshwater, oligohaline, and mesohaline is also greater in summer than spring and fall. There is also a regional pattern in $NO_3$ and $NH_4$ concentrations; for example, the polyhaline region always exhibits significantly lower $NO_3$ concentrations than the other regions.

Focusing on results from the model experiments, C:Chla in Models 1 and 2 exhibit seasonal and regional variability (Fig. 5). For instance, in winter, spring, and fall, Model 1 has the optimal value of C:Chla increasing as the regions become more saline and further away from the tributaries. Model 2 has the same pattern, except in fall where the highest ratio is in the mesohaline region. The model skill does not change between the two models, except in bias where Model 1 performs better than Model 2 during spring and fall (Fig. 6). It is also worth noting that in both models, the polyhaline region performs worse during summer and fall than

`

in winter and spring. This pattern was also present in the correlation and RRSD (not shown).

For the nitrogen limitation experiment, the optimal values for $\overline{K_{NO_3}}$ were usually at the maximum value of 5 mmol-N $m^{-3}$ or near the minimum value of 0 mmol-N $m^{-3}$, with only oligohaline in the spring and freshwater region in summer having values near the reference constant of 0.5 mmol-N $m^{-3}$ (Fig. 7). In contrast, all of the optimal $\overline{K_{NH_4}}$ values in Model 3 were lower than the reference value of 0.5 mmol-N $m^{-3}$. These lower values of $K_{NH4}$ result in less nitrogen limitation (cf., values of $L_{NO3} + L_{NH4}$ closer to 1) in Model 3 than in Model 1 (Fig. 8). The nitrogen limitation term in the polyhaline region increased the most between the two models (from 0.67 to 0.94).

Model 3's bias in all four regions during the summer are less negative than Model 1 (from -18.8 mgC $m^{-3}$ $h^{-1}$ to -0.3 mgC $m^{-3}$ $h^{-1}$). However, the bias in the freshwater and oligohaline regions is larger in Model 3 during the spring and autumn (spring: from -21.9 mgC $m^{-3}$ $h^{-1}$ to -26.0 mgC $m^{-3}$ $h^{-1}$, fall: from -10.4 mgC $m^{-3}$ $h^{-1}$ to -31.9 mgC $m^{-3}$ $h^{-1}$; Fig. 9). Model 3 also has an improved bias in the polyhaline region in summer and fall compared to Model 1 (summer: from -6.5 mgC $m^{-3}$ $h^{-1}$ to -3.3 mgC $m^{-3}$ $h^{-1}$, fall: from -11.3 mgC $m^{-3}$ $h^{-1}$ to -3.8 mgC $m^{-3}$ $h^{-1}$; Fig. 9). However, the RRSD does not show significant differences between Model 1 and Model 3 in the polyhaline region during all four seasons (Fig. 10), with the skill still decreasing in both models from spring to fall (spring: 0.82, fall: 0.88). We also do not find significant differences in RRSD between Model 1 and 3 when focusing on the other regions except for the freshwater region in fall (from 0.71 to 0.82). Correlation also had a similar result, with the overall skill barely changing between Model 1 and Model 3, and no change in skill present for the polyhaline region (not shown).

## Discussion

We expected the lowest C:Chla ratios to exist in the freshwater and oligohaline regions during the spring, where turbidity tends to be higher (St-Laurent and Friedrichs, 2024). Our results reflect this pattern (Fig. 5), with optimal values increasing further away from the tributaries, a pattern expected based on observed turbidity concentrations. This may suggest that we should cluster our data based on TSS, and possibly implement a TSS dependence in our C:Chla parameterization. The seasonal and regional variability seen in both models might also be linked to our hypothesis, which was that these

`

different regions at different times of the year have a different optimal model parameter because of their unique phytoplankton characteristics.

There was also seasonal and regional variability in the optimal parameter values for $\sqrt{K_{NO_3}}$ and $\sqrt{K_{NH_4}}$ in Model 3, where lower values in both parameters correspond to less nitrogen limitation, and very high values for $\sqrt{K_{NO_3}}$ only result in $NH_4$ limitation. With these values set to 0.5 mmol-N $m^{-3}$, the model has a large summer bias because it is too nutrient limiting. This bias is later removed when there is no limitation placed on the model during summer, which was the case in Model 3.

Moving onto model skill, our findings from the first model experiment concluded that both maximum algal growth rates result in approximately the same performance. Similarly, the optimal values for $\sqrt{K_{NO_3}}$ and $\sqrt{K_{NH_4}}$ only altered the bias of the model, whereas Correlation and RRSD remained the same between Model 1 and Model 3, even though the values in Model 3 were mostly much higher or lower than the original values in Model 1. This shows that the current PP model has low sensitivity to changes in model parameters. Thus, we did not find strong indicators that we have to change the maximum algal growth rate or the nitrogen limitation term in our current PP model because our experiments did not improve the model skill.

The simplicity of the current model may explain the model's low sensitivity to change in model parameters, and more complexity may potentially result in better model skill. One aspect we may want to add in the future is a TSS dependence in C:Chla in order to account for photoacclimation. In this study we tuned C:Chla for each season and region to partially capture photoacclimation, but turbidity can change on time scales shorter than the seasons, for example with spring and neap tides (Cerco *et al.,* 2004).

We may also try altering the model to account for vertical migration and mixotrophy. Dinoflagellates *Prorocentrum minimum,* and *Margalefindinium polykrikoides*, which have been observed since the start of the continuous monitoring in the Chesapeake Bay in 1985 (Marshall *et al*., 2009), are known to vertically migrate and acquire heterotopic carbon through grazing on phytoplankton, also known as mixotrophy (Mulholland *et al*., 2018). Our study already shows a decrease in bias when optimizing the half-saturation constants, adding vertical migration and mixotrophy may yield more dramatic improvements in model skill.

`

## Figures

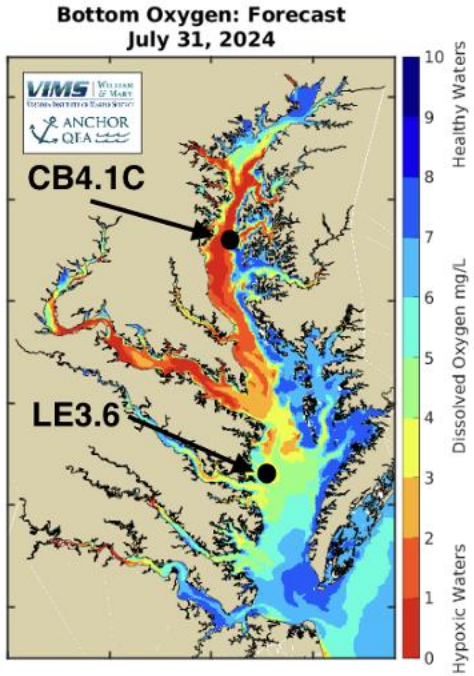


Figure 1: Forecast of bottom oxygen (mg/L) for 31 July 2024 generated using the Chesapeake Bay Environmental Forecast System (https://www.vims.edu/cbefs).

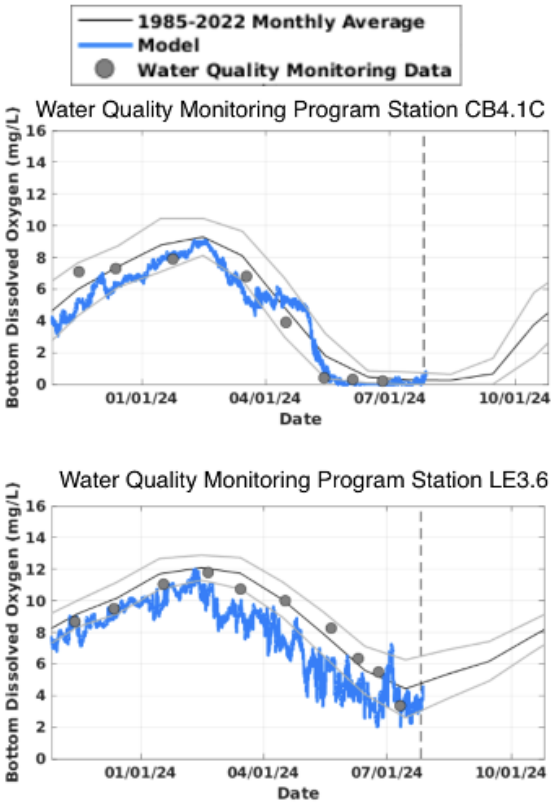


Figure 2: Modeled (blue curve) and observed (dots) bottom dissolved oxygen concentration at station CB4.1C (top) and LE3.6 (bottom) for Oct.-July 2024 (figure from CBEFS, 2024). The gray and black curve indicate the 1985-2022 average and standard deviation, respectively. indicate the 1985-2022 average and standard deviation, respectively.

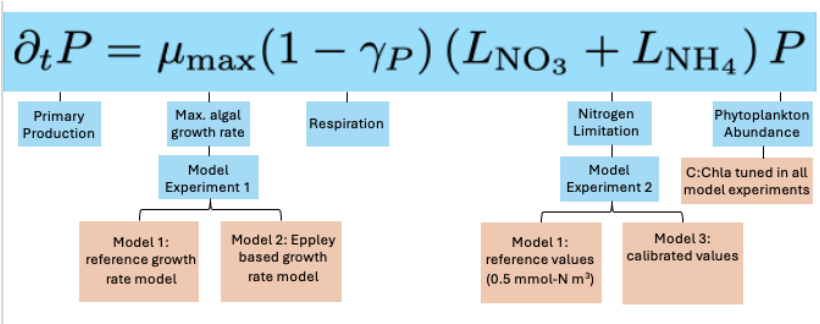


Figure 3: Schematic overview of our approach to test whether an alternative temperature dependence of the maximum growth rate (Model 2) or refining the nutrient limitation (Model 3) improves the skill of our current primary production model (Model 1; see Methods for further information)

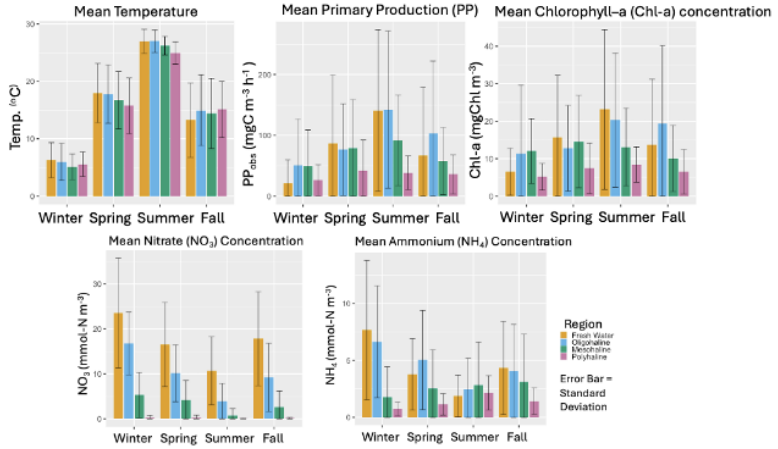


Figure 4: Averaged observations of water temperature (Temp), primary production ($PP_{obs}$), Chlorophyll-a (Chla), nitrate ($NO_3$), and ammonium ($NH_4$) for various seasons and salinity regions in the Chesapeake Bay between 1984-2009.

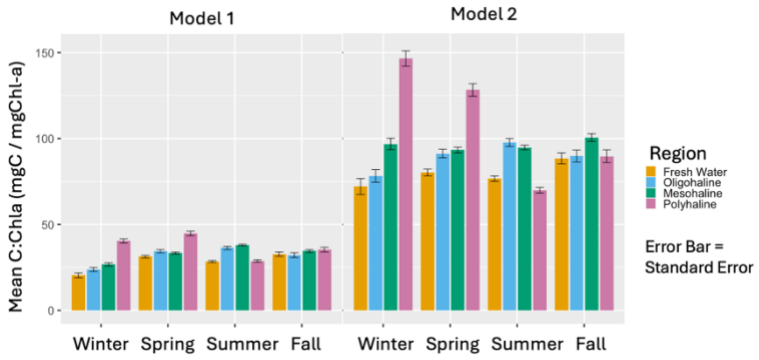


Figure 5: Averaged tuned carbon-to-Chlorophyll-a (C:Chla) ratios for various seasons and salinity regions using Model 1(left) and Model 2(right).

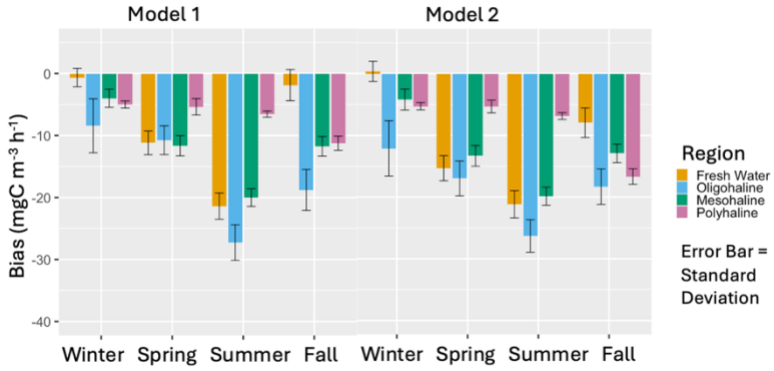


Figure 6: Averaged bias of Model 1 (left) and Model 2 (right) for various seasons and salinity regions.

`

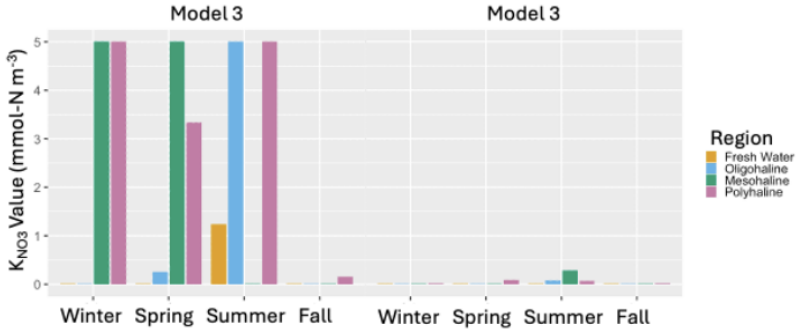


Figure 7: Averaged optimal half-saturation values of nitrate ($K_{NO3}$) (left) and ammonium ($K_{NH4}$) (right) for Model 3 for various seasons and salinity regions.

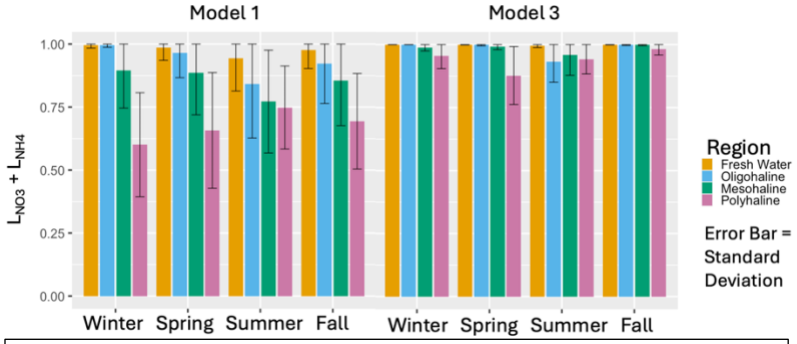


Figure 8: Averaged total nitrogen limitation function value ($L_{NO3} + L_{NH4}$) of Model 1 (left) and Model 3 (right) for various seasons and salinity regions.

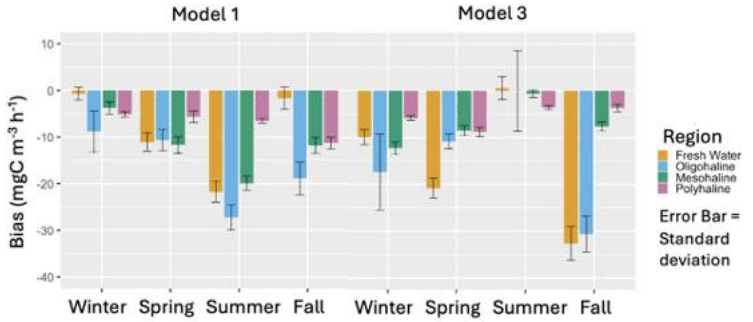


Figure 9: Averaged bias of Model 1 (left) and Model 3 (right) for various seasons and salinity regions.

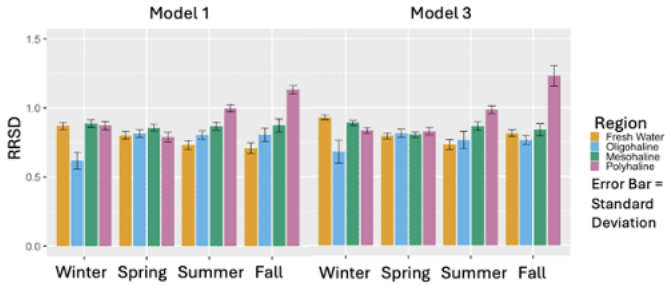


Figure 10: Averaged relative root square difference (RRSD) of Model 1 (left) and 3 (right) for various seasons and salinity regions.

`

**Acknowledgements**

I thank my mentors, Dante M.L. Horemans, Pierre St-Laurent, & Marjorie A.M. Friedrichs, for helping me with my research this summer. I would also like to acknowledge graduate student Olivia Szot for creating the maximum algal growth rate model that was used as a reference model for my research.

Thanks to Stephanie Peart for serving as the REU teaching assistant. Program funding for the VIMS Research Experience for Undergraduates was made available through a grant awarded from the National Science Foundation (grant # NSF OCE 1659656) to Drs. Rochelle Seitz and Grace Massey.

Part of this work was funded by the National Oceanic and Atmospheric Administration Coastal Ocean and Modeling Testbed Project under award NA21NOS0120167 to Virginia Institute of Marine Science, William & Mary.

`

**Literature Cited**


Batiuk, Richard. Dear Rich, Enclosed is the STAC scientific review of the Bay Program's Ambient Water Quality Criteria for Dissolved Oxygen, Water Clarity and Chlorophyll a for the Chesapeake Bay and Tidal Tributaries (DRAFT). The document was reviewed by 10 scientists with four from institutions from outside the Bay watershed.

Bever, A. J, Friedrichs, M.A., & St-Laurent, P. 2021. Real-time environmental forecasts of the Chesapeake Bay: Model setup, improvements, and online visualization. Environmental Modelling & Software, 140, 105036

CBEFS. 2024. Dissolved Oxygen Line Plots and Model-Data Comparison. Virginia Institute of Marine Science. Retrieved June 27, 2024, from https://www.vims.edu/research/products/cbefs/do_lineplots/

Cerco, C.F., & Noel, M.R. 2004. Process-based primary production modeling in Chesapeake Bay. Marine Ecology Progress Series, 282, 45-58.

Chavez, F. P., Messié, M., & Pennington, J. T. 2011. Marine primary production in relation to climate variability and change. Annual Review of Marine Science, 3, 227-260.

Cloern, J. E. 2001. Our evolving conceptual model of the coastal eutrophication problem. Marine Ecology Progress Series, 210, 223-253.

Diaz, R. J., & Rosenberg, R. 2008. Spreading dead zones and consequences for marine ecosystems. Science, 321(5891), 926-929.

Eppley, R.W. 1971. Temperature and phytoplankton growth in the sea. Fishery bulletin, 70(4), 1063.

Hagy, J. D., Boynton, W. R., Keefe, C. W., & Wood, K. V. 2004. Hypoxia in Chesapeake Bay, 1950–2001: long-term change in relation to nutrient loading and river flow. Estuaries, 27, 634-658.

Harding Jr, L.W., Meeson, B.W., & Fisher Jr, T.R. 1986. Phytoplankton production in two east coast estuaries: photosynthesis-light functions and patters of carbon assimilation in Chesapeake and Delaware Bays. Estuarine, Coastal and Shelf Science, 23(6), 773-806.

Irby, I.D., Friedrichs, M.A., Da, F., & Hinson, K. E. 2018. The competing impacts of climate change and nutrient

reductions on dissolved oxygen in Chesapeake Bay. Biogeosciences, 15(9), 2649-2668.

Kemp, W. M., Boynton, W. R., Adolf, J. E., Boesch, D. F., Boicourt, W. C., Brush, G., ... & Stevenson, J. C. 2005. Eutrophication of Chesapeake Bay: historical trends and ecological interactions. Marine Ecology Progress Series, 303, 1-29.

Marshall, H. G., Lane, M.F., Nesius, K. K., & Burchardt, L. 2009. Assessment and significance of phytoplankton species composition within Chesapeake Bay and Virginia tributaries through a long-term monitoring program. Environmental monitoring and assessment, 150, 143-155.

Mulholland, Margaret R., Morse, R., Egerton, T., Bernhardt, P.W., & Filippino, K. C. (2018). Blooms of dinoflagellate mixotrophs in a lower Chesapeake Bay tributary: carbon and nitrogen uptake over diurnal, seasonal, and interannual timescales. Estuaries and Coasts, 41, 1744-1756.

Nixon, S. W. 1995. Coastal marine eutrophication: a definition, social causes, and future concerns. Ophelia, 41(1), 199-219.

Parker, R. A. 1993. Dynamic models for ammonium inhibition of nitrate uptake by phytoplankton. Ecological Modelling, 66(1-2), 113-120.

Seitz, R. D., Dauer, D. M., Llansó, R. J., & Long, W. C. 2009. Broad-scale effects of hypoxia on benthic community structure in Chesapeake Bay, USA. Journal of Experimental Marine Biology and Ecology, 381, S4-S12.

St-Laurent Pierre, Friedrichs Marjorie A. M. 2024. An atlas for physical and biogeochemical conditions in the Chesapeake Bay. SEANOE. https://doi.org/10.17882/99441

St-Laurent, P., & Friedrichs, M. A. M. 2024. On the sensitivity of coastal hypoxia to its external physical forcings. Journal of Advances in Modeling Earth Systems, 16(1), e2023MS003845.